Food Biophysics (2025) 20:68
https://doi.org/10.1007/s11483-025-09957-8

RESEARCH

Inhibition Effects of Some Phenolic Anthraquinone Derivatives on Lactoperoxidase Activity: A Detailed in Vitro and in Silico investigation

Işıl Nihan Korkmaz[1] · **Halil Şenol**[2] · **Ramazan Kalın**[3]

Received: 5 February 2025 / Accepted: 3 April 2025 / Published online: 11 April 2025

Abstract

The basic nutrient of all living beings in the developmental age is milk. Milk contains many things necessary for ideal nutrition. One of the enzymes found in bovine milk is lactoperoxidase (LPO; EC 1.11.1.7). The LPO system functions as a natural defense system, especially in newborn babies. Despite the many benefits of milk, contamination of breast milk with environmental toxins is common. Over time, people accumulate a lifetime load of chemicals from drugs to environmental pollutants, and these can be passed on to the baby during breastfeeding. Anthraquinones are colorful compounds that can be produced both naturally and synthetically. These compounds are widely used in industry and medicine due to their biological activities and colorful structures. In this study, in vitro enzyme inhibition study, molecular docking and molecular dynamics (MD) simulation parameters were examined to investigate the inhibitory potential of anthraquinone derivatives, which are widely used as coloring agents, against the lactoperoxidase enzyme. The inhibitors showed competitive inhibition with K_i values between 0.4964 ± 0.042–2.0907 ± 0.1044 µM. 1,2-Dihydroxy-anthraquinone was predicted to have the highest affinity on the LPO receptor, with estimated free binding energies of -7.11 kcal/mol. The stability of both ligand and protein, as shown by the low RMSD and RMSF values, shows that 1,2-dihydroxy-anthraquinone **(2)** maintains strong and stable interactions throughout the MD simulation, further supporting the high binding affinity and potential biological activity of the compound. We hope that this study will guide the development of drugs targeting the LPO enzyme with anthraquinone derivatives.

Keywords Lactoperoxidase · Anthraquinone · Molecular docking · Molecular dynamics (MD) simulations

Introduction

The increasing population of living beings in the world brings about rapid industrialization. The wastes and toxic chemical emissions resulting from rapidly increasing industrial activities such as paper, paint, cosmetics, medicine, leather, textile and food cause negative effects on human health [1–3]. Although a wide variety of components are used in the industry, dyes are a component that has constant use [4, 5]. Dyes, which have a wide range of uses and are used in different sectors, provide coloring of objects by interacting with the material to be dyed [6–8]. In this context, food dyes used in additives used in the food industry are used for various purposes such as protecting and increasing the desired and original color, standardizing the appearance by preventing color change and deterioration, increasing the appeal and creating new products. Food dyes are also used in confectionery, snacks, beverages, cakes and gelatin desserts [9–11].

✉ Işıl Nihan Korkmaz
isil.krkmz@gmail.com; nihan.korkmaz@alparslan.edu.tr

Halil Şenol
hsenol@bezmialem.edu.tr

Ramazan Kalın
ramazan.kalin@erzurum.edu.tr

[1] Faculty of Applied Sciences, Department of Plant Production and Technologies, Muş Alparslan University, Muş 49250, Turkey

[2] Faculty of Pharmacy, Department of Pharmaceutical Chemistry, Bezmialem Vakif University, Fatih, İstanbul 34093, Turkey

[3] Department of Basic Science, Faculty of Science, Erzurum Technical University, Erzurum 25050, Turkey

Flavones, flavonols, anthraquinones and indigotin compounds contained in plants and insects used in different areas as dyes and pigments are known as natural dyes [12–16]. Flavonoids and anthraquinones are the two main groups of natural dyes [17–21]. Anthraquinones have been used in different areas due to their colorful structures and biological activities. Anthraquinone derivatives with biological properties, both synthetic and natural anthraquinones, are widely used in pesticides, dyes, textile dyeing, foods, imaging devices, pharmaceuticals and cosmetics [22–27].

Depending on their areas of use, people are under the influence of thousands of xenobiotics from the air, soil, water and food they take. Therefore, any toxic substance that enters the biological system can be metabolized. In recent years, it has been known that chemicals and toxic substances that enter the metabolism of living beings are transmitted to breast milk as a result of metabolic processes [28].

Lactoperoxidase (LPO), naturally secreted into milk, is an enzyme that plays an important role against pathogenic microorganisms in relation to the defense mechanism in the digestive system of newborn babies [29, 30]. Found in milk; Lactoperoxidase (LPO), which protects the intestinal tract and mammary glands of newborns against pathogenic microorganisms, is an oxidoreductase that plays a role in suppressing and inhibiting the growth of bacteria in metabolism [31, 32]. In summary, LPO acts as a natural defense mechanism in biotransformation against pathogens [33]. Accordingly, biological systems can act on a toxic compound in a variety of ways. Biochemical change occurs through the action of enzymes and is concluded with the inhibition or alteration of a particular metabolic pathway.

Our primary aim in this study is not to deliberately inhibit lactoperoxidase (LPO) but rather to investigate the potential effects of anthraquinone derivatives on this enzyme. Anthraquinones, whether naturally occurring or synthetically produced, are widely used in various industries, including food, cosmetics, and textile manufacturing, due to their coloring properties and biological activities. As a result, these compounds can inadvertently enter the human body through dietary intake, cosmetic applications, or environmental exposure.

Given that LPO plays a crucial role in the body's natural defense system, especially in newborns, understanding how these commonly encountered anthraquinone derivatives interact with this enzyme is of significant importance. Our study aims to evaluate whether these compounds, which may be present in maternal milk due to bioaccumulation over time, have any inhibitory effects on LPO. This is particularly relevant because exposure to environmental toxins through breastfeeding is a growing concern, and elucidating their potential impact on LPO activity could contribute to a better understanding of their biological consequences.

In this study, anthraquinone derivatives, including anthraquinone **(1)**, 1,2-dihydroxyanthraquinone **(2)**, 1,5-dihydroxyanthraquinone **(3)**, 2,6-dihydroxyanthraquinone **(4)**, 1,8-dihydroxy-3-methylanthraquinone **(5)**, and 1,4-dihydroxy-2,3-dimethylanthraquinone **(6)** (Fig. 1), were investigated to determine their inhibitory effects on lipid peroxidation (LPO) in vitro, alongside molecular docking and molecular dynamics studies to elucidate the underlying inhibition mechanisms.

Materials and Methods

Materials

All chemicals used within the scope of the study were supplied from Sigma-Aldrich and Merck.

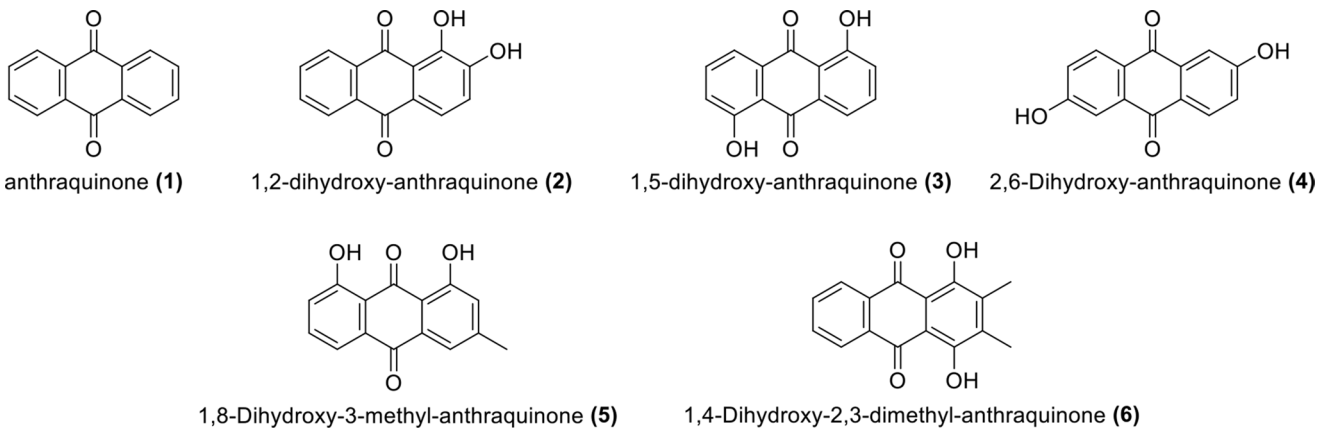

Fig. 1 The chemical structure of quinones used in this study

Purification of LPO

The bovine milk used in the study was purchased from a local dairy in Erzurum province. LPO was isolated from milk as in our previous study. First, the affinity matrix was synthesized by modifying the method we used in our previous study by binding sulfanilamide as the ligand and LTyrosine as CNBr to the activated Sepharose-4B. CNBr activated Sepharose-4B was washed with cold $NaHCO_3$ buffer (100 mM, pH: 10.0) and transferred to a beaker. L-Tyrosine was bound to CNBr activated Sepharose 4B. The reaction was stirred for 90 min. The mixture was washed with distilled water to remove excess L-Tyrosine from the Sepharose 4B-L-Tyrosine gel. LPO was purified in a single step by this Sepharose-4B-L-Tyrosine-sulfanilamide column chromatography. All purification steps were performed at 4 °C. In the first step, the affinity column was equilibrated with phosphate buffer (10 mM, pH 6.8), bovine milk homogenate was washed with phosphate buffer (25 mM, pH 6.8) and then loaded onto the column. LPO was then eluted with $NaCl/Na_2HPO_4$ (1.0 M/0.25 M, pH 6.8) enzyme solution. Protein flux in the column eluates was determined spectrophotometrically at 280 nm. Eluants from the column were lyophilized, then dialyzed overnight against equilibrated buffers and finally protein concentration was determined. Previous studies have reported The lyophilization process in detail [34].

Determination of LPO Activity

LPO activities were determined according to the procedure of Shindler and Bardsley with a minor modification [35]. This method is based on the oxidation of ABTS (2,20 -azino-bis (3-ethylbenzthiazoline-6 sulfonic acid) diammonium salt) as a chromogenic substrate by H_2O_2(hydrogen peroxide), which results in a product that absorbs at 412 nm. The one unit of activity is defined as the amount of enzyme catalyzing the oxidation of 1 µmol of ABTS min^{-1} at 25 °C (molar absorption coefficient 32,400 M^{-1} cm^{-1}) [36].

Inhibition Kinetics of Anthraquinone Derivatives

Inhibition kinetics of anthraquinone and its derivatives IC_{50} values were determined from the graphs drawn as a result of experimental studies on the LPO enzyme at least five different inhibitor concentrations [37, 38]. After IC_{50} values were determined from the graphs, Lineweaver and Burk's curves were drawn at three different inhibitors and five different substrate concentrations. From these graphs, the K_i value and inhibition types of each inhibitor were determined separately [39].

Computational Studies

Molecular docking studies were performed using Schrödinger's Maestro (14.3) interface, while MD simulations were conducted with Desmond (D. E. Shaw Research) via Maestro Interface (14.3).

Preparation of Ligands and Proteins

The protein and ligand preparation followed protocols established by our research group. The three-dimensional structures of the target proteins were obtained from the Protein Data Bank (PDB) via the RCSB platform (https://www.rcsb.org). Bovine lactoperoxidase (PDB ID: 3R4X) was selected for all computational analyses. Protein preparation and optimization were performed using Schrödinger's Maestro 14.3, including bond order adjustments, ionization state assignments, and removal of water molecules to ensure accurate docking [40, 41].

Glide Docking and İnduced Fit Docking

We performed Glide and Induced Fit Docking (IFD) following previously published methods. Each ligand was docked into the target receptor using Schrödinger's IFD workflow (Schrödinger Release 2025-1). The Glide grid was centered on the native ligand's centroid, with the outer grid set to 25 Å. For flexible docking, 20 poses per ligand were generated and evaluated using Glide XP for enhanced accuracy. The resulting IFD docking scores were used to assess binding affinity and prioritize the best poses for further analysis [42, 43].

Prime MM-GBSA Analysis

Prime MM-GBSA analysis was performed using Schrödinger Suite 2025-1, following protocols from our previous studies. Binding free energies were calculated with the MM-GBSA module, using the VSGB solvation model and minimized sampling. Flexible conformational adjustments were allowed for residues near the active site, while surrounding regions were restrained. This method provided accurate binding energy estimates, reflecting the stability and affinity of the ligand-protein complexes [44, 45].

Molecular Dynamics Simulations

MD simulations were performed using Desmond (D.E. Shaw Research) featuring Maestro Interface 2025-1, following the previously published protocols. The protein-ligand complex was initially prepared with the System Builder module, where it was placed in a orthorhombic box with

a 10 Å buffer zone. The system was solvated using TIP4P water molecules, and NaCl was added to a physiological concentration of 0.15 M to maintain neutrality. Energy minimization was carried out with the OPLS4 force field to accurately represent molecular interactions. The simulation was conducted for 500 ns under NPT conditions (300 K, 1 atm) with a 500 ps time step. Protein-ligand interactions, including hydrogen bonds, hydrophobic contacts, and salt bridges, were analyzed throughout the simulation. The stability and dynamic behaviors of the complex was evaluated by monitoring the RMSD, RMSF, H bond, SASA, rGry, MolSA and PSA analysis [46, 47].

Docking Validations

In this study, re-docking was used to validate the docking results. The co-crystal ligand, pyrazine-2-carboxamide, was extracted from the target enzyme (3R4X) and re-docked onto its respective receptor. The binding pose quality was assessed using RMSD, with values below 2 Å considered reliable. Superposition of the re-docked ligand with the crystal structure was also performed to visually confirm the accuracy of the binding pose [48].

Results and Discussion

Enzyme Inhibition and Kinetic Study

LPO is an enzyme found in milk and has many potential applications such as food preservation, milk and cheese industries, as it reduces microflora. LPO is also biologically important because it has a natural defense system against bacterial growth and micro-organisms. Some chemicals and drugs change normal enzyme activities with specific enzyme inhibitions [49].

IC_{50} values were determined from the activity measurements of anthraquinone derivatives across different dose ranges. The IC_{50} and K_i values for compounds **1–6** were calculated, and the results are presented in Table 1. In addition to the IC_{50} values, the K_i values, which reflect the binding affinity of the compounds, were also determined. The inhibition types of the anthraquinone derivatives were assessed using Lineweaver-Burk plots [39]. These values provide a comprehensive understanding of the inhibitory potential of each compound, with both the IC_{50} and K_i data contributing to the overall evaluation of their effectiveness [39].

Table 1 Inhibition data of anthraquinone derivatives

Compound	R^2	IC_{50} (μM)	K_i (μM)	Inhibition type
Anthraquinone **(1)**	0.9395	0.397	0.496 ± 0.042	Competitive
1,2-dihydroxy-anthraquinone **(2)**	0.9111	0.361	0.561 ± 0.022	Competitive
1,5-dihydroxy-anthraquinone **(3)**	0.9111	1.447	2.090 ± 0.104	Competitive
2,6-Dihydroxy-anthraquinone **(4)**	0.9569	0.764	1.314 ± 0.212	Competitive
1,8-Dihydroxy-3-methyl-anthraquinone **(5)**	0.9835	0.728	1.236 ± 0.055	Competitive
1,4-Dihydroxy-2,3-dimethyl-anthraquinone **(6)**	0.9382	2.003	1.415 ± 0.464	Competitive

The inhibition data of the anthraquinone derivatives show varying levels of inhibitory potency, as measured by the IC_{50} and *K*i values, with all compounds demonstrating competitive inhibition. Compounds **1** and **2**, with IC_{50} values of 0.397 μM and 0.361 μM, respectively, exhibit the strongest inhibition, supported by their relatively low *K*i values of 0.496 ± 0.042 μM and 0.561 ± 0.022 μM. These compounds are the most effective in inhibiting the enzyme, suggesting strong binding affinity and potency. Compound **3**, with a higher IC_{50} of 1.447 μM and *K*i of 2.090 ± 0.104 μM, shows significantly weaker inhibition, making it the least potent of the series. Similarly, compounds **4** and **5** demonstrate moderate inhibition, with IC_{50} values of 0.764 μM and 0.728 μM, and *K*i values of 1.314 ± 0.212 μM and 1.236 ± 0.055 μM, respectively. These compounds display a good correlation between concentration and inhibition, with high R^2 values of 0.9569 and 0.9835, but their potency is lower compared to compounds **1** and **2**. Compound **6**, with an IC_{50} value of 2.003 μM and *K*i of 1.415 ± 0.464 μM, is the weakest inhibitor in this series. Overall, the data indicates that compounds **2** is the most promising candidate for further development.

Anthraquinone derivatives have been shown to inhibit various enzymes, including Paraoxonase-1 (PON1), lactate dehydrogenase (LDH), and acetylcholinesterase (AChE). Studies revealed IC_{50} and K_i values in the range of 3.27–82.90 μM and 2.50 ± 0.65 to 30.90 ± 7.20 μM for PON1 inhibition, with competitive inhibition observed. Similarly, anthraquinone derivatives demonstrated competitive inhibition of LDH and AChE, with *K*i values ranging from 0.014 to 0.123 μM, emphasizing their potential as therapeutic inhibitors [50–53].

The IC_{50} graphs are provided in Fig. 2, while the corresponding K_i graphs are presented in Fig. 3. These figures illustrate the inhibitory effects of the anthraquinone derivatives, with Fig. 2 showing the dose-response curves used to calculate IC_{50} values, and Fig. 3 presenting the K_i values, which further highlight the binding affinities of the compounds.

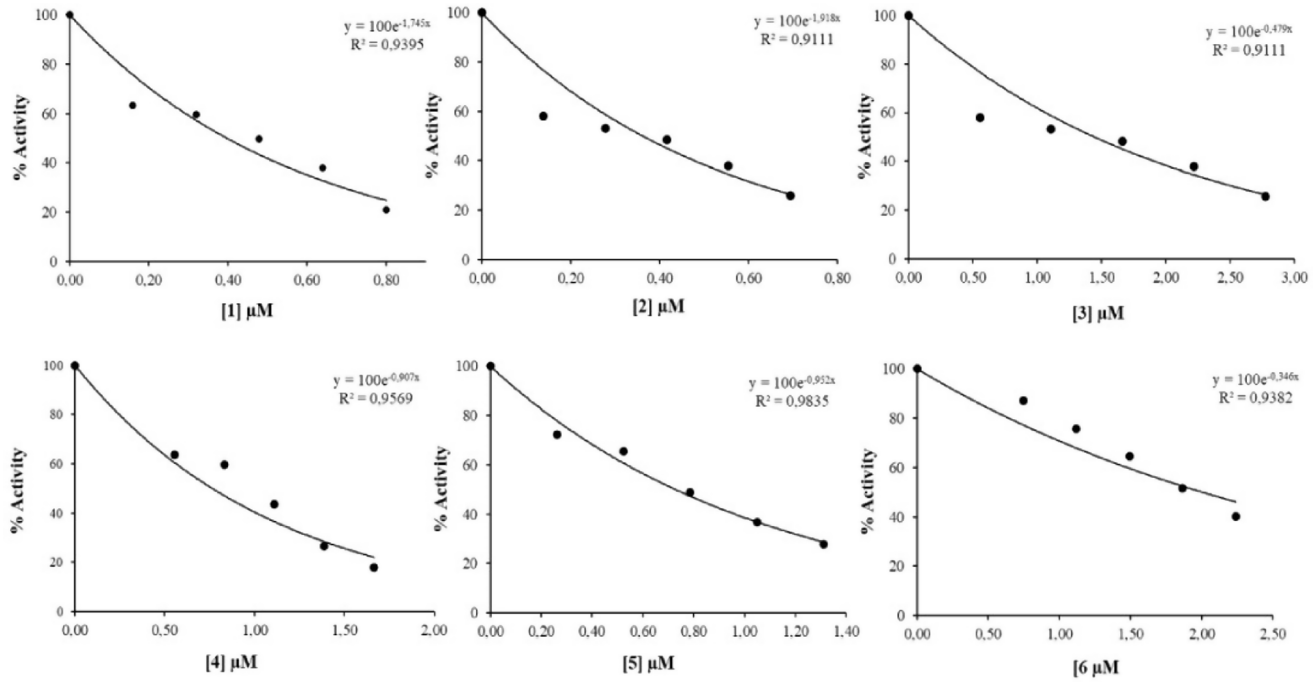

Fig. 2 Activity(%)-[Inhibitor] graphs for LPO enzyme obtained by molecules depending on ABTS substrate

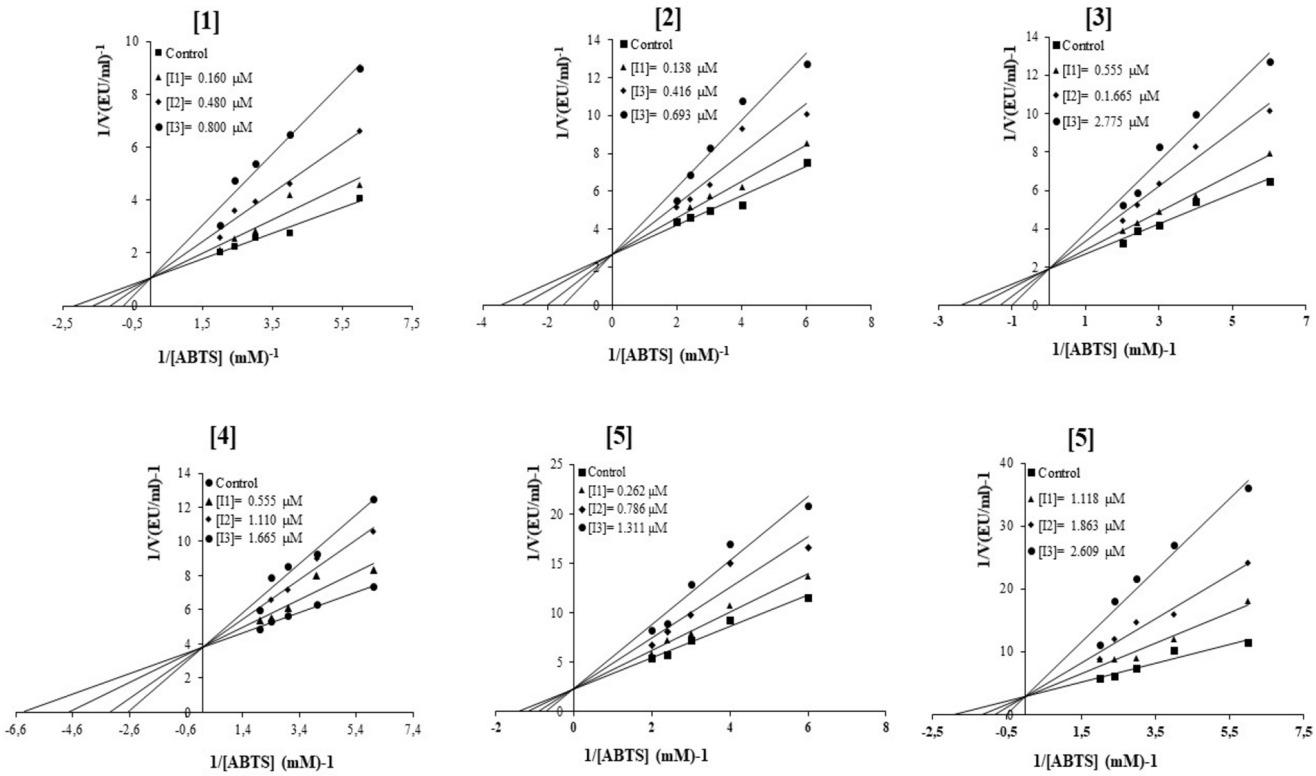

Fig. 3 1/V (EU/ml.)$^{-1}$and 1/[ABTS] (mM)$^{-1}$ graphs for LPO enzyme obtained with molecules depending on ABTS substrate

Molecular Docking Studies

Molecular docking is an important tool in drug discovery, enabling the study of ligand-protein binding interactions and affinities. Induced Fit Docking (IFD) technic enhances precision by allowing the protein to adjust to the ligand's shape, creating a more realistic binding model. The MM-GBSA (Molecular Mechanics-Generalized Born Surface Area) method further refines this analysis by calculating binding free energy, combining molecular mechanics with solvation effects to quantify interaction strength and stability [54, 55].

In this study, molecular docking was employed to explore the potential inhibitory mechanisms of anthraquinone derivatives by examining their binding interactions with the active site of the lactoperoxidase enzyme. Docking studies were specifically conducted on the enzyme's active site, as all derivatives exhibited competitive inhibition in the in vitro enzyme kinetic studies. The docking process utilized the IFD approach and binding free energies (ΔG) were determined using the MM-GBSA method. The findings are summarized in Table 2.

The results indicate that 1,2-dihydroxy-anthraquinone **(2)** is the most potent inhibitor of the lactoperoxidase enzyme. It demonstrated a low K_i value (0.561 µM), indicating strong in vitro inhibitory potency, along with a favorable docking score (-7.110 kcal/mol) and a robust MM-GBSA ΔG binding energy (-41.96 kcal/mol), reflecting high binding affinity and complex stability. While the parent compound, anthraquinone **(1)**, showed the lowest K_i value (0.496 µM), its less favorable docking score (-5.224 kcal/mol) and MM-GBSA ΔG bind (-32.98 kcal/mol) suggest weaker binding interactions compared to compound **2**. Other derivatives, such as 2,6-dihydroxy-anthraquinone **(4)** and 1,4-dihydroxy-2,3-dimethyl-anthraquinone **(6)**, displayed strong MM-GBSA ΔG bind values (-48.27 kcal/mol and −41.53 kcal/mol, respectively), but their higher *K*i values and moderate docking scores indicate reduced potency. The evaluation of 1,5-dihydroxy-anthraquinone **(3)** and 1,8-dihydroxy-3-methyl-anthraquinone **(5)** provides additional insights into their inhibitory potential. Compound **3** exhibited a relatively high K_i value (2.091 µM), indicating lower in vitro potency compared to other derivatives. However, it achieved a moderately favorable docking score (-6.804 kcal/mol) and MM-GBSA ΔG binding energy (-30.94 kcal/mol), suggesting it forms stable but less potent interactions with the active site of the lactoperoxidase enzyme. In contrast, compound **5** showed a better K_i value (1.236 µM), indicating higher inhibitory potency than compound **3**. It also achieved a strong docking score (-7.118 kcal/mol), comparable to the most potent derivatives, which suggests good binding affinity. However, its MM-GBSA ΔG binding energy (-24.78 kcal/mol) was the least favorable among all compounds, indicating lower stability of the ligand-protein complex. The reference drug, Sulfanilamide, is included in the docking study as a comparative inhibitor. Its docking score is -4.514 kcal/mol, indicating a lower binding affinity to the target compared to the anthraquinone derivatives. The MMGBSA ΔG bind for sulfanilamide is -8.05 kcal/mol, suggesting a relatively weaker binding interaction with the enzyme target in comparison to the anthraquinone compounds, which exhibit more negative values, indicating stronger binding affinity.

Table 2 Docking scores and MM-GBSA ΔG binding free energies of the anthraquinone and derivatives against lactoperoxidase enzyme (PDB ID: 3R4X)

No	Compound Name	Docking score (kcal/mol)	MMGBSA ΔG Bind (kcal/mol)
1	Anthraquinone	-5.224	-32.98
2	1,2-Dihydroxy-anthraquinone	-7.110	-41.96
3	1,5-Dihydroxy-anthraquinone	-6.804	-30.94
4	2,6-Dihydroxy-anthraquinone	-6.738	-48.27
5	1,8-Dihydroxy-3-metil-anthraquinone	-7.118	-24.78
6	1,4-Dihydroxy-2,3-dimetil-anthraquinone	-7.316	-41.53
7	Sulfanilamide (reference inhibitor) [56]	-4.514	-8.05

The molecular docking two dimensional (2D) ligand protein interactions of all derivatives are given in Fig. 4. As shown in Fig. 4, all target compounds interact with the protoporphyrin ring in the active site of the lactoperoxidase (LPO) enzyme. The interaction between the protoporphyrin ring and inhibitors in LPO is a key element of the inhibition mechanism. Since the protoporphyrin ring is part of the heme group in the active site of LPO, the binding of inhibitors to this ring directly affects the enzyme's catalytic activity. Inhibitors that interact with the protoporphyrin ring disrupt the oxidation-reduction cycle of the iron atom, preventing the production of reactive oxygen species by the enzyme. The binding of inhibitors to the protoporphyrin ring destabilizes this critical structure, potentially halting or weakening LPO's function, thus inhibiting its biological and pharmaceutical effects [34].

All the anthraquinone derivatives interact with the protoporphyrin ring through π-π stacking and/or π-cationic interactions. In addition to the protoporphyrin interactions in all compounds, Fig. 4a shows that the carbonyl group of compound **1** forms a hydrogen bond with Arg-225 and a π-π stacking interaction with His-109.

Figure 4b demonstrates that the hydroxyl groups of compound **2** form three different hydrogen bonds with Gln-105, Asp-109, and His-109, while also interacting with Arg-225 through a π-cationic interaction. In Fig. 4c, the ketone and hydroxyl groups of compound **3** simultaneously form two

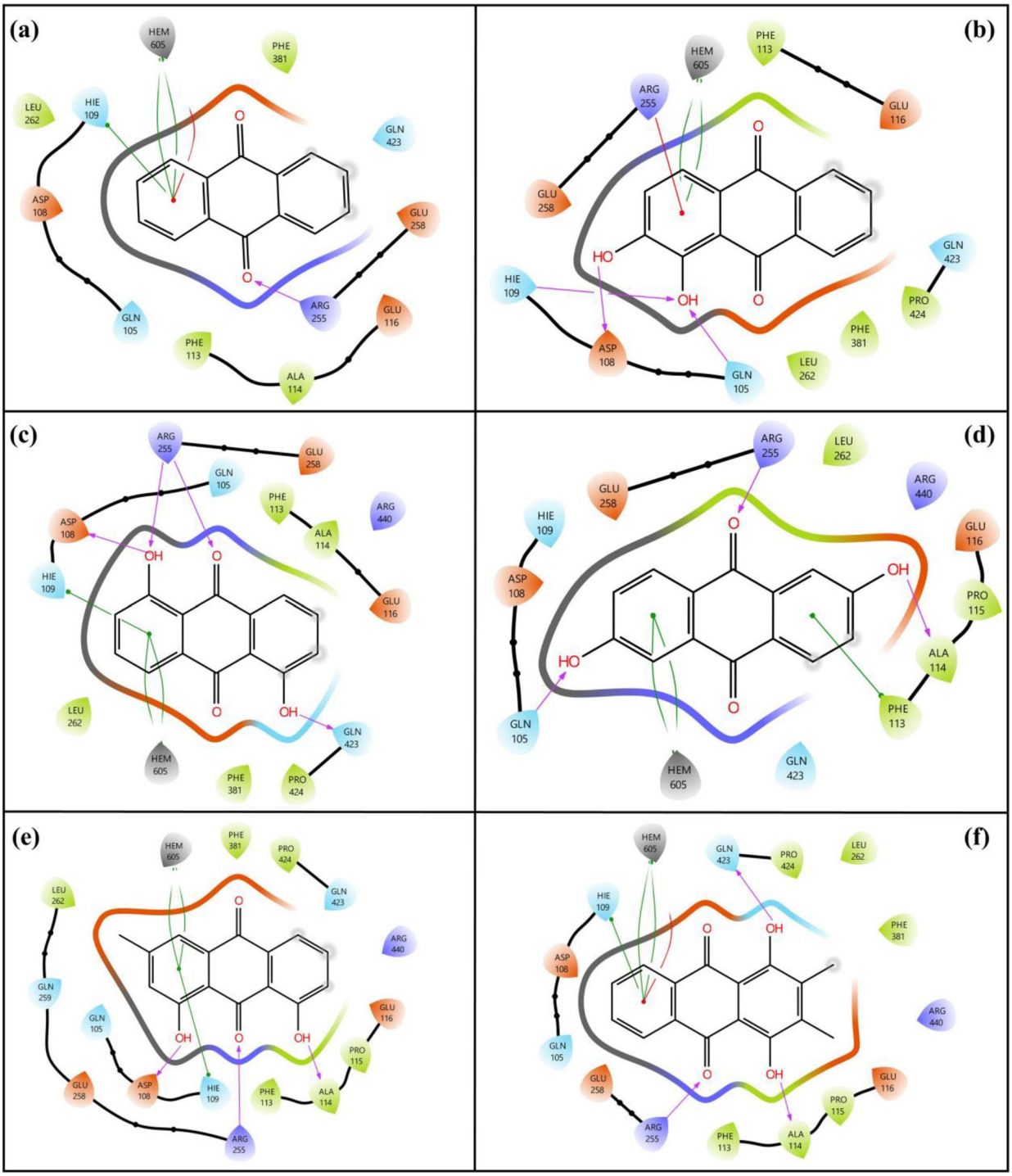

Fig. 4 Molecular docking 2D ligand protein interactions (LPI) between anthraquinone derivatives and lactoperoxidase (LPO) enzyme. (**a**) LPI of **1-LPO** complex, (**b**) LPI of **2-LPO** complex, (**c**) LPI of **3-LPO** complex, (**d**) LPI of **4-LPO** complex, (**e**) LPI of **5-LPO** complex and (**f**) LPI of **6-LPO** complex

hydrogen bonds with Arg-225, while the same hydroxyl group also forms an additional hydrogen bond with Asp-108. Other hydroxyl group in the molecule forms another hydrogen bond with Gln-423. In Fig. 4d, the ketone group of compound **4** forms a hydrogen bond with Arg-225, while the hydroxyl groups interact with Gln-105 and Ala-114 through hydrogen bonding. Additionally, π-π stacking interaction with Phe-113 is observed. In Fig. 4e, the ketone group of compound **5** forms a hydrogen bond with Arg-225, and the hydroxyl groups at C1 and C8 positions form two separate

hydrogen bonds with Asp-108 and Ala-114, respectively. Moreover, a π-π stacking interaction with His-109 is noted. Finally, in Fig. 4f, the ketone group of compound **6** forms a hydrogen bond with Arg-225, while the hydroxyl groups form two additional hydrogen bonds with Gln-423 and Ala-114. Compound exhibits π-π stacking interactions with the heme core, along with π-cationic interactions. Additionally, a π-π stacking interaction with His-109 is also present. The molecular docking three dimensional (3D) ligand protein interactions of all derivatives are given in Fig. 5. In Fig. 5 the pink structure represents the protoporphyrin ring. The yellow dashes represent the hydrogen bond interactions, the turquoise dashes represent the π-π stacking interactions and the red dashes represent the π-cationic interactions. Additionally, the red sphere in the middle of the protoporphyrin ring represents the iron atom.

As shown in Fig. 5, the ligands are stacked parallel to the protoporphyrin ring within the active site of the enzyme, forming interactions with it. The gray clouds in the Fig. 5 represent the protein's surface binding areas, while the bluish clouds indicate the ligand surface binding area. When the ligand fully occupies the active site, the surface binding areas overlap completely, signifying that the ligand is thoroughly accommodated in the active site of the enzyme. This complete binding enhances the inhibitory potential of the ligand and increases the stability of the ligand-protein complex. Additionally, as seen in Fig. 5, the hydrogen bond lengths range from 2.0 to 2.40 Å, with shorter hydrogen bonds indicating a more stable ligand-protein complex. This strong binding suggests that the inhibitor candidates exhibit high binding affinity, contributing to their effectiveness in inhibiting the enzyme.

As conclusion the interactions between anthraquinone derivatives and the protoporphyrin ring of lactoperoxidase are key to their inhibitory potential. π-π stacking and π-cationic interactions with the protoporphyrin ring stabilize the binding of these inhibitors, disrupting the enzyme's catalytic activity by affecting the heme group's function. Additionally, hydrogen bonding with key residues like Arg-225, His-109, Asp-108, Gln-105, and Ala-114 further strengthens the binding and impairs the enzyme's normal function. The combination of these interactions indicates a strong binding affinity, making the anthraquinone derivatives promising candidates for developing potent lactoperoxidase inhibitors with potential therapeutic applications.

Molecular Dynamics (MD) Simulations

Molecular Dynamics (MD) simulations track atomic movements to study molecular interactions and behavior. In drug discovery, MD helps predict binding affinity, explore conformational changes, and optimize drug candidates. Key parameters like RMSD (Root Mean Square Deviation) assess complex stability, while RMSF (Root Mean Square Fluctuation) measures protein flexibility, aiding in the evaluation and optimization of potential drugs [40, 44]. Based on in vitro testing and molecular docking results, 1,2-dihydroxy-anthraquinone **(2)** emerges as the most promising candidate. Although for all derivatives 500 ns MD simulation studies were carried out the MD simulation analysis of **2-LPO** complex is evaluat[[34[[34ed. The MD simulation analysis of **2-LPO** complex is presented in Fig. 6, while the MD simulations for other complexes can be found in the supporting materials.

Figure 6a represents the 2D key ligand-protein interactions (LPI) along with the simulation time percentages, emphasizing the importance of certain interactions over the course of the simulation. The phenolic hydrogen forms a hydrogen bond with Asp-108 during 94% of the simulation time, which is highly significant as it indicates a strong, consistent interaction, essential for maintaining the stability of the ligand-protein complex throughout the simulation. This extended interaction time suggests that the bond with Asp-108 is a key stabilizing factor in the complex. Similarly, another phenolic OH group interacts with Gln-105 via a hydrogen bond for 81% of the simulation time, also indicating a long-lasting and important interaction that likely contributes to the stability and specificity of the binding. In comparison, the other interactions, such as those with the carbonyl oxygen (11%) and the π-π stacking interactions with His-109 and Phe-113 (18% and 15%, respectively), while still important, occur less frequently, suggesting secondary stabilizing roles. These findings underscore the importance of the primary hydrogen bonds in ensuring strong and consistent ligand binding during the simulation.

Figure 6b represents the RMSD of the ligand and protein Cα atoms throughout the simulation, providing insight into the structural stability and conformational changes. The average RMSD of the protein Cα atoms is 1.2 Å (pale blue), indicating a relatively stable protein structure with only slight deviations from its initial conformation during the simulation. The average RMSD of the ligand when fit onto the protein is 1.0 Å, suggesting that the ligand maintains a stable position within the protein binding site, with minimal movement or deviation. In contrast, the average RMSD of the ligand fit onto its initial position (0.20 Å, pink) reflects very little deviation from its starting position, indicating that the ligand remains highly stable and closely adheres to its original orientation throughout the simulation.

Figure 6c and d show the RMSF of protein Cα atoms and ligand atoms, reflecting the flexibility of both during the simulation. The average RMSF of the protein Cα atoms is 0.8 Å, indicating minimal fluctuation and structural stability. The ligand's average RMSF is 0.6 Å, suggesting it remains

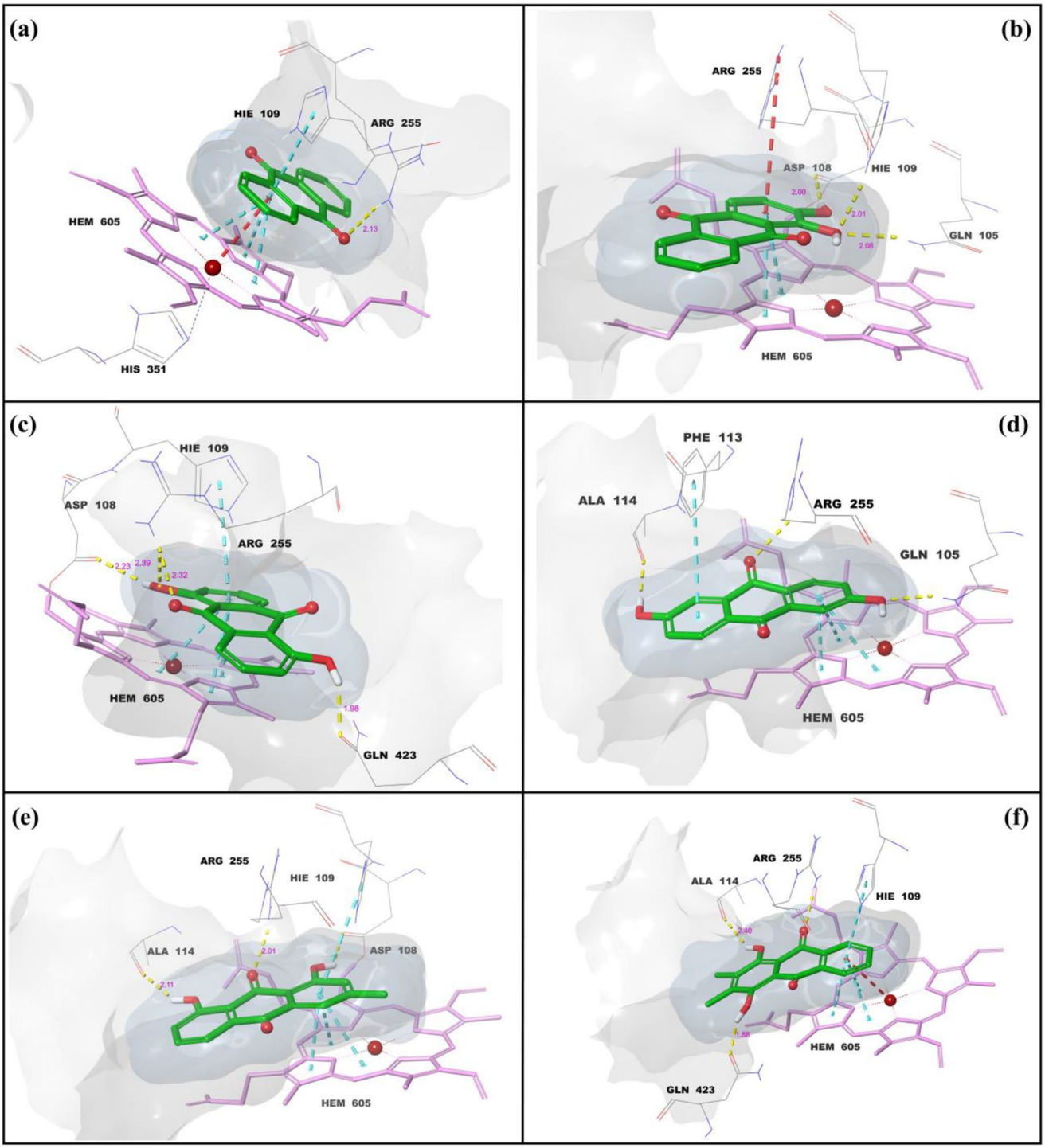

Fig. 5 Molecular docking 3D ligand protein interactions (LPI) and surface binding analysis between anthraquinone derivatives and lactoperoxidase (LPO) enzyme. (**a**) LPI of **1-LPO** complex, (**b**) LPI of **2-LPO** complex, (**c**) LPI of **3-LPO** complex, (**d**) LPI of **4-LPO** complex, (**e**) LPI of **5-LPO** complex and (**f**) LPI of **6-LPO** complex

stable within the binding site. Figure 6c also highlights 14 amino acid contacts (represented by green vertical lines), confirming that the ligand maintains consistent interactions with the protein throughout the simulation, further supporting the stability of the ligand-protein complex. Figure 6e represents the fractional interaction histogram, which summarizes the interactions between the ligand and the protein. Since a functional group can interact with multiple amino acid residues and a single residue can engage with several functional groups, all fractional interactions are accumulated

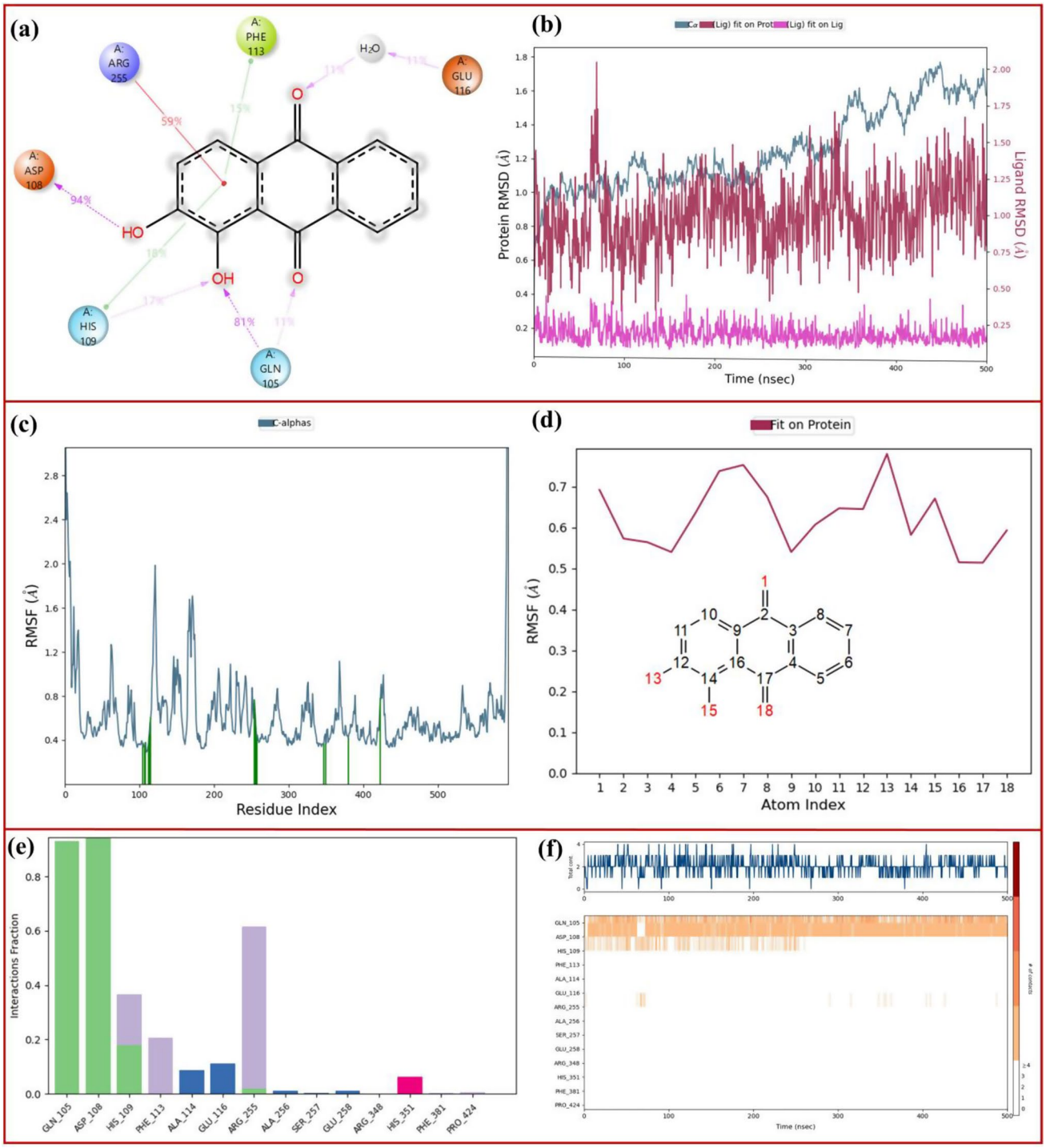

Fig. 6 The MD simulation analysis of **2-LPO** complex. (**a**) 2D key ligand protein interactions, (**b**) RMSD of ligand and protein atoms, (**c**) RMSF of protein atoms, (**d**) RMSF of ligand atoms and (**e**) fractional interaction histograms (**f**) H bond timeline depiction

to create this histogram. The histogram is color-coded to differentiate the types of interactions: green for hydrogen bonds, blue for water-mediated hydrogen bonds, purple for hydrophobic interactions, and red for ionic interactions. The y-axis indicates the relative interaction ratio, reflecting the frequency of each interaction type. The most abundant fractional interactions are observed with the residues Gln-105, Asp-108, and Arg-255, highlighting the key roles these amino acids play in stabilizing the ligand-protein complex. Finally, Fig. 6f shows the hydrogen bond (H-bond) interaction timeline, illustrating the interactions between the ligand and key amino acid residues. Asp-108, Gln-105, His-109,

and Arg-255 form hydrogen bonds with the ligand during the simulation. Asp-108 and Gln-105 exhibit stable hydrogen bond interactions, with their bonds lasting throughout most of the simulation. In contrast, His-109 forms hydrogen bonds for approximately 40% of the simulation, while Arg-255's interaction is more transient, occurring only between 3 and 5% of the simulation time. This timeline highlights the varying stability of these interactions, with Asp-108 and Gln-105 playing more significant roles in stabilizing the ligand-protein complex compared to His-109 and Arg-255.

The molecular dynamics simulation rGyr, MoISA, SASA, and PSA values graphs are given in Fig. 7. As seen in Fig. 7, The RMSD fluctuates between 0.2 and 0.6 Å, indicating that the structure remains close to its initial conformation without significant large-scale structural changes. The Radius of Gyration *(rGyr)* stays within a narrow range of 3.36–3.54 Å, reflecting stable compactness and minimal overall shape changes. The intramolecular hydrogen bonds *(intraHB)* occur infrequently, with sporadic spikes, suggesting that internal hydrogen bonding is transient and not a primary stabilizing factor. The Molecular Surface Area *(MoISA)* remains relatively steady between 210 and 215 Å2, indicating constant surface exposure, while the Solvent-Accessible Surface Area *(SASA)* fluctuates within 125–150 Å2, with minor spikes likely due to small conformational shifts. Similarly, the Polar Surface Area *(PSA)* stays between 150 and 165 Å2, showing stable solvent exposure of polar regions throughout the simulation. The overall trends suggest that the system is well-equilibrated and structurally stable, with minimal perturbations. If this simulation involves a ligand-protein complex, the stability of PSA and SASA values may indicate consistent ligand binding, while the low occurrence of intraHB suggests a potential preference for intermolecular interactions.

MD Simulation Validation and Reproducibility

To verify the MD simulation results and calculate standard deviations, the MD simulation of the **2-LPO** ligand-protein complex was performed in triplicate using random seed. RMSD and RMSF graphs obtained from the random seed MD simulation analysis are given in Fig. 8 as combined. In addition, the average values of the RMSD and RMSF graphs obtained from the random seed MD simulations are given in Fig. 8, and the comparison of these values with the custom seed is given in Table 3.

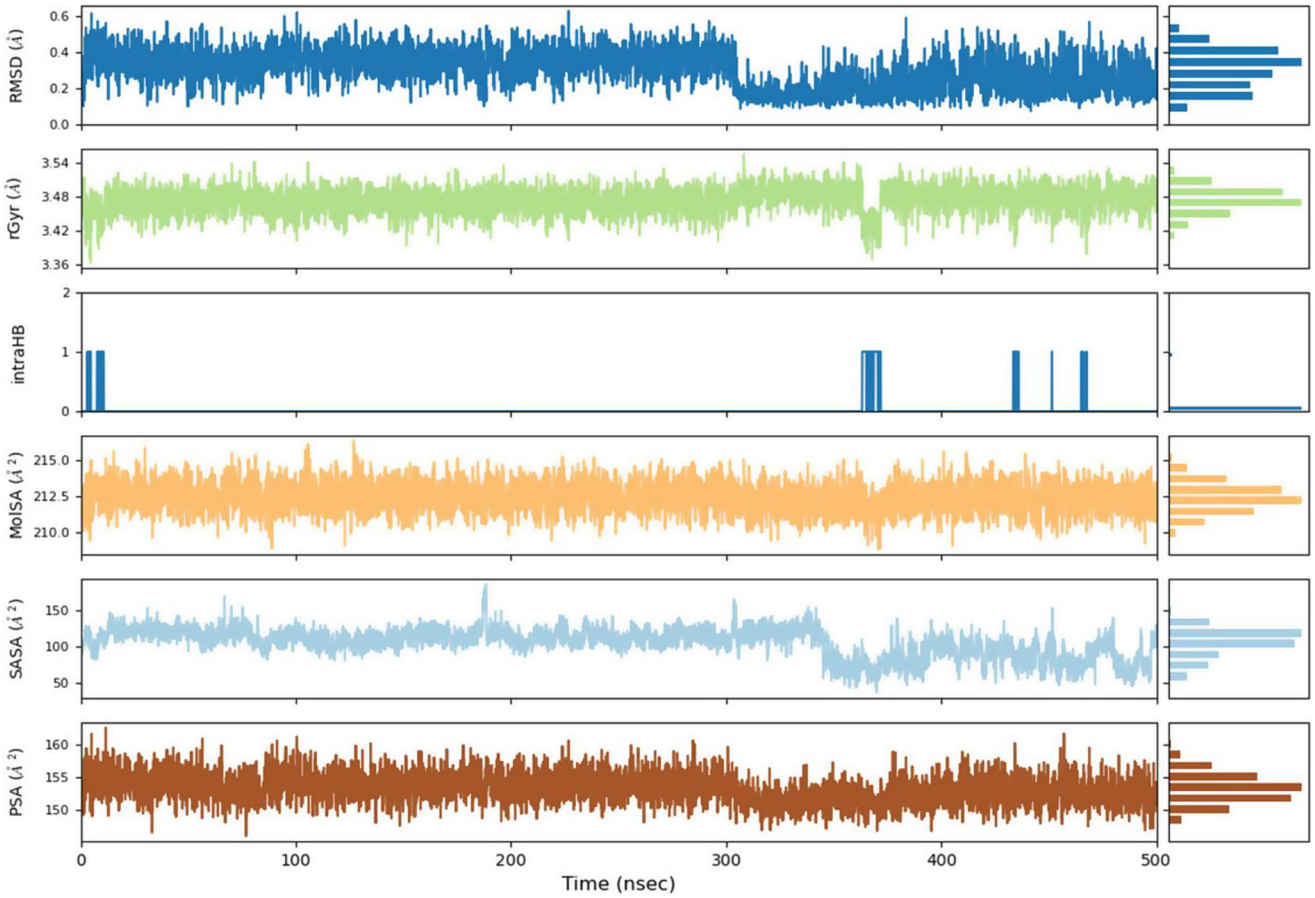

Fig. 7 Molecular dynamics simulation RMSD, rGyr, MoISA, SASA, and PSA values

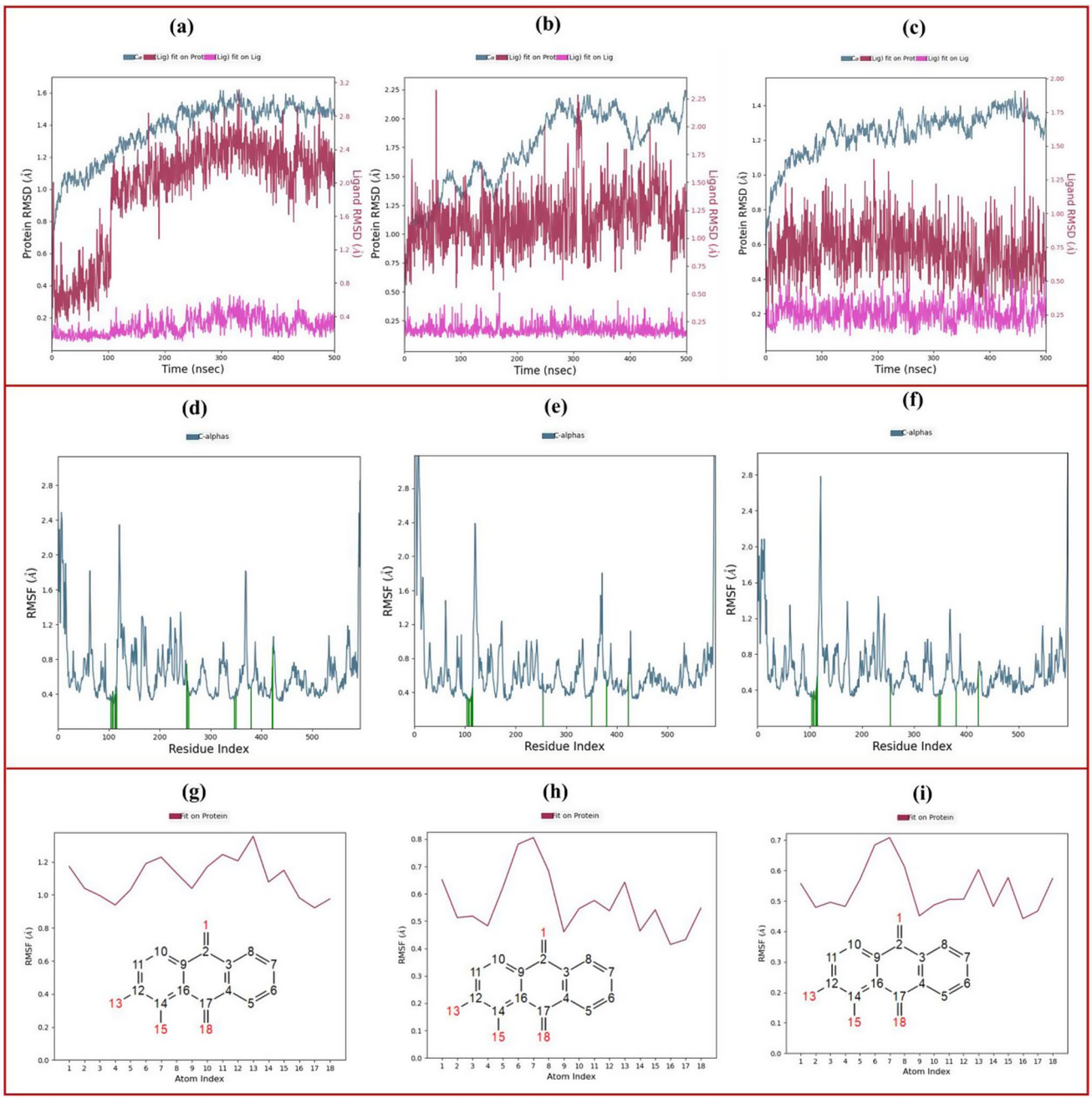

Fig. 8 In triplicate Random Seed (RS) MD simulation analysis of **2-LPO** complex. (**a**) RMSD of protein and ligand atoms for RS1, (**b**) RMSD of protein and ligand atoms for RS2, (**c**) RMSD of protein and ligand atoms for RS3, (d) RMSF of protein atoms for RS1, (**e**) RMSF of protein atoms for RS2, (**f**) RMSF of protein atoms for RS3, (**g**) RMSF of ligand atoms for RS1, (**h**) RMSF of ligand atoms for RS2 and **(i)** RMSF of ligand atoms for RS3

Table 3; Fig. 8 compare the RMSD and RMSF values of protein and ligand atoms in the **2-LPO** complex using random seeds and a custom seed. The results show that both the random seeds and the custom seed yield similar values, confirming the reliability of the simulation. For RMSD of Protein Cα atoms, the values range from 1.10 to 1.60 Å for random seeds, with an average of 1.30 Å, and 1.20 Å for the custom seed. RMSD of Ligand fit on Protein averages 1.00 Å for both, and RMSD of Ligand fit on Ligand shows minimal deviation (0.20–0.30 Å). RMSF values for protein and ligand atoms are also consistent, with slight differences in ligand RMSF (random seeds: 0.55–1.10 Å, custom seed: 0.60 Å), but overall, the results are closely aligned. This consistency demonstrates that the custom seed provides stable and reproducible results, similar to those from random seeds.

Table 3 MD simulation custom and random seed average RMSD and RMSF values of protein and ligand atoms of **2-LPO** complex

	Random Seed 1	Random Seed 2	Random Seed 3	Average of Random Seeds	Custom Seed
RMSD of Protein Cα Atoms	1.20	1.60	1.10	1.30	1.20
RMSD of Ligand fit on Protein	1.70	1.25	0.75	1.00	1.00
RMSD of Ligand fit on Ligand	0.30	0.20	0.25	0.25	0.20
RMSF of Protein Cα Atoms	0.80	0.82	0.84	0.82	0.80
RMSF of Ligand Atoms	1.10	0.60	0.55	0.75	0.60

Comparison of Reference Inhibitor with Anthraquinone Derivatives

Figure 9 illustrates the molecular docking and molecular dynamics (MD) simulation analyses of sulfanilamide, a reference inhibitor, and its comparison with anthraquinone derivatives. Figure 9a illustrates the 2D LPI from molecular docking, where sulfanilamide's amino group forms a hydrogen bond with Ala-114 and the HEM group, while the benzene ring engages in two π-π stacking interactions with HEM. These interactions demonstrate the key binding modes of sulfanilamide with the protein. Figure 9b shows the 3D representation of the molecular docking interactions, where yellow lines represent hydrogen bonds and turquoise lines depict π-π stacking interactions. Sulfanilamide is well-positioned within the binding surface, indicating a stable binding pose within the active site.

Figure 9c provides the 2D key LPI from molecular dynamics simulations, showing that the sulfonamide amino group maintains a 97% hydrogen bond interaction with Ala-114, and the sulfonyl oxygen forms a 78% hydrogen bond with Glu-116. Additionally, Arg-255 contributes to 13% of water-mediated hydrogen bonds. The phenyl ring exhibits 91% π-π stacking interaction with Phe-113, and 29% π-cationic interaction with Arg-348. These results suggest stable and significant interactions of sulfanilamide with key amino acids in the protein. In comparison, compound **2** exhibits similar interactions, such as hydrogen bonds with Glu-116, Phe-113, and Arg-255, demonstrating that the anthraquinone derivatives interact with these residues similarly to sulfanilamide, reinforcing the relevance of these amino acids in the binding mode.

Figure 9d shows the RMSD values, with the average RMSD of protein Cα atoms being 1.0 Å (pale blue), and the average RMSD of the ligand at 1.8 Å (red), indicating slight fluctuations in the ligand position. The RMSD of ligand deviation from its initial position is 0.2 Å, indicating relatively stable binding for sulfanilamide. However, compound **2** shows a lower RMSD and a more stable complex, suggesting that the anthraquinone derivative forms a more stable interaction than sulfanilamide.

Figure 9e and f present the RMSF values for the protein and ligand atoms, with average values of 0.8 Å and 0.7 Å, respectively, indicating low flexibility of both the protein and ligand during the simulation, which is favorable for stable binding. Finally, Fig. 9g shows the fractional interaction histogram, highlighting the key amino acids involved in the interaction: Phe-113, Ala-114, and Glu-116. These residues play crucial roles in the binding and stabilization of sulfanilamide in the active site. When comparing sulfanilamide to the **2-LPO** complex, compound **2** show more stable and consistent binding interactions, indicated by lower RMSD values and more compact ligand positioning. While sulfanilamide forms strong interactions, particularly with residues Ala-114, Glu-116, and Phe-113, the anthraquinone derivatives exhibit more pronounced stability, with a distinct and more consistent interaction profile with key amino acids.

Molecular Docking Validation

The co-crystal (pyrazine-2-carboxamide) ligand of lactoperoxidase (PDB ID: 3R4X) was re-docked at their actual crystal positions without changing their states or producing any conformers, thereby validating the molecular docking methods and protocols. The original crystallographic conformation was superimposed with the co-crystallized ligand's docked pose, and the RMSD were found to be 0.1491 Å. Docking validation images are given in (Fig. 10).

Conclusion

In this study, we aimed to explore the inhibition effects of various anthraquinone derivatives on lactoperoxidase (LPO) activity, not as a deliberate inhibitor of LPO but to understand their potential interaction with the enzyme. Our results indicate that anthraquinone derivatives, particularly compound **2** (1,2-dihydroxyanthraquinone), exhibit significant inhibitory activity on LPO, with a low K_i value (0.561 μM), suggesting strong binding affinity and potent in vitro inhibition. This compound also demonstrated favorable molecular docking scores (-7.110 kcal/mol) and stable MM-GBSA ΔG binding energies (-41.96 kcal/mol), confirming its potential as the most effective inhibitor in this study.

The in vitro inhibition data showed that compounds **1** (anthraquinone) and **2** were the most potent inhibitors, with IC_{50} values of 0.397 μM and 0.361 μM, respectively. These results were corroborated by molecular docking and dynamics simulations, which revealed that the anthraquinone derivatives form strong interactions with key amino acid residues in the LPO active site, particularly through π-π

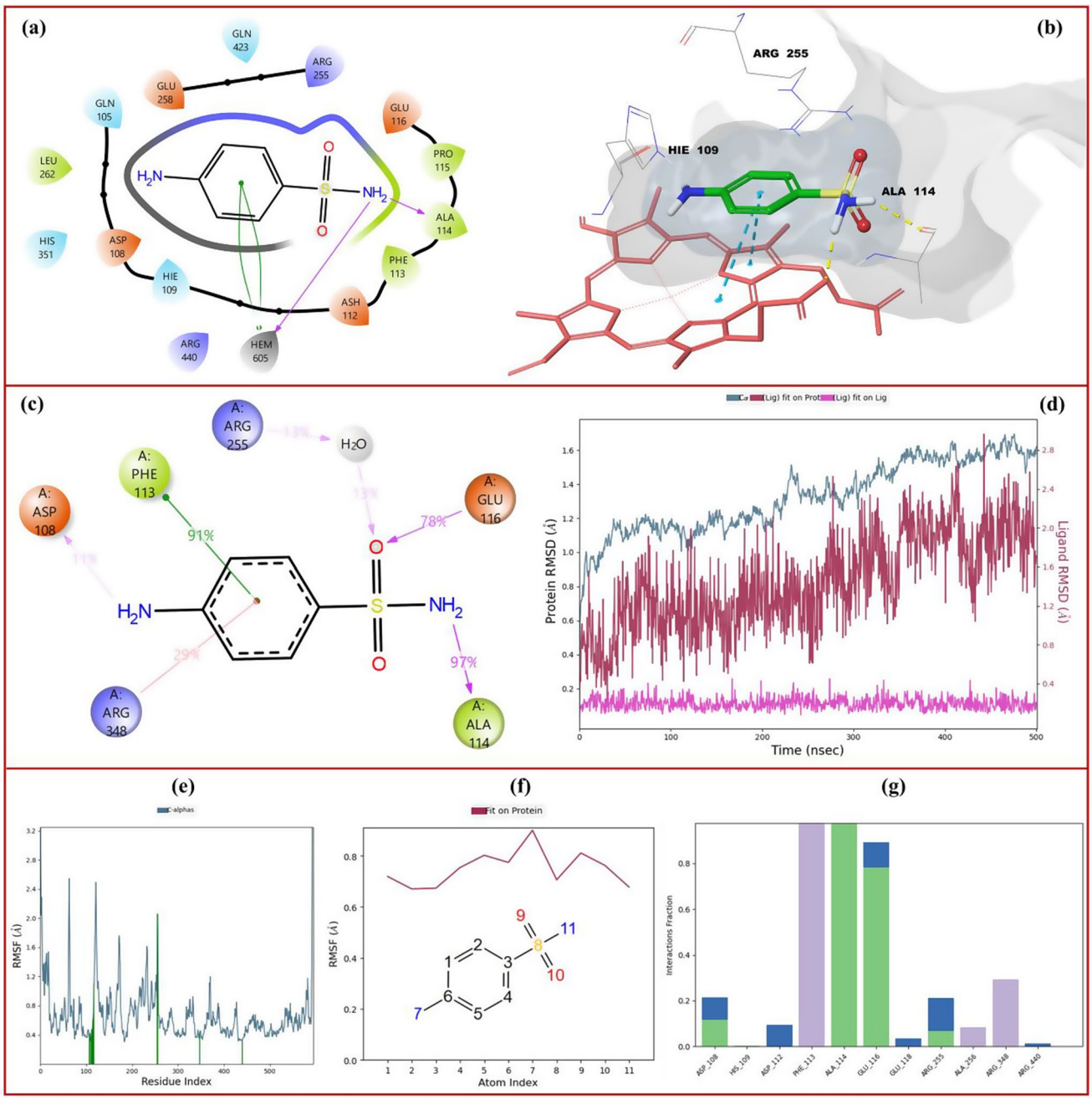

Fig. 9 Molecular docking and molecular dynamics analysis of reference inhibitor sulfanilamide. (**a**) molecular docking 2D LPI, (**b**) molecular docking 3D LPI, (**c**) MD simulation 2D key LPI, (**d**) RMSD values of ligand and protein atoms, (**e**) RMSF of protein Cα atoms, (**f**) RMSF of ligand atoms and (**g**) fractional interaction histogram

stacking and hydrogen bonding with residues like Arg-225, His-109, Asp-108, Gln-105, and Ala-114. These interactions disrupt the enzyme's catalytic activity, primarily by affecting the function of its heme group, which is crucial for its peroxidase activity.

The molecular dynamics simulations demonstrated that the ligand-protein complex remains stable over time, with minimal RMSD and RMSF fluctuations, indicating a well-formed and stable binding between the anthraquinone derivatives and the LPO enzyme. The analysis of the fractional interaction histogram highlighted key residues like Asp-108 and Gln-105, which had the most consistent interactions with the ligand, further stabilizing the complex. The consistent values of Radius of Gyration (rGyr), Molecular Surface Area (MoISA), and Solvent-Accessible Surface Area (SASA) suggest that the ligand is well-equilibrated within the binding site, with minimal conformational changes during the simulation.

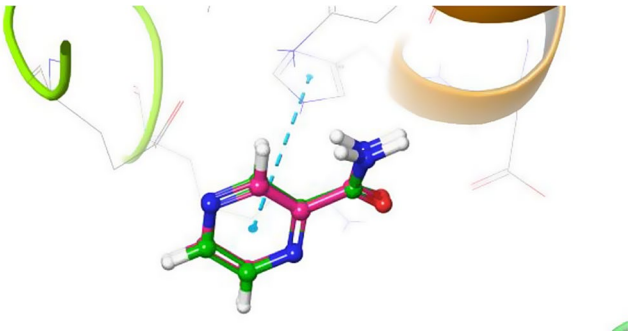

Fig.10 The green color represents the co-crystal while pink represents re-docked pose (Docking validation images)

Comparing the docking results of sulfanilamide, a reference inhibitor, with compound **2** shows that the latter exhibits stronger binding interactions, demonstrated by more stable RMSD values and more compact ligand positioning within the active site. Sulfanilamide, while forming strong interactions with residues like Ala-114, Glu-116, and Phe-113, shows weaker binding affinity compared to the anthraquinone derivatives, particularly compound 2.

Overall, our study provides valuable findings the inhibitory effects of phenolic anthraquinone derivatives on LPO, highlighting compound **2** as the most promising candidate for further development. The combination of in vitro assays, molecular docking, and molecular dynamics simulations reveals a complex and stable interaction between the anthraquinone derivatives and LPO, making them strong candidates for therapeutic applications as potent LPO inhibitors. The findings of this study are significant, particularly regarding the inhibition of lactoperoxidase (LPO). LPO plays a crucial role in the immune defense system, especially in the protection of mucosal surfaces, such as the breast tissue. Inhibiting LPO activity could impair the natural defense mechanisms, making it an undesirable effect, especially when considering potential exposure through maternal milk. Since LPO is involved in the antimicrobial defense of infants, compounds that inhibit its activity could negatively affect the newborn's immune system. This emphasizes the importance of the current findings, as they highlight the potential risks associated with the inadvertent exposure to these anthraquinone derivatives, especially in populations such as infants, where immune protection is vital.

Author Contributions I. N. Korkmaz: Conceptualization, investigation, writing-original draft and methodology. H. Şenol: Conceptualization, investigation, software, methodology, and writing-original draft. R. Kalın: Conceptualization and formal analysis. All authors read and approved the final manuscript.

Funding Open access funding provided by the Scientific and Technological Research Council of Türkiye (TÜBİTAK).

Data Availability No datasets were generated or analysed during the current study.

Declarations

Informed Consent Not applicable.

Competing Interests The authors declare no competing interests.

References

1. B. Demiralp, İ. Büyük, S. Aras, D. Cansaran, Duman, Industrial and biotechnological applications of laccase enzyme. Turkish Bull. Hygiene Experimental Biology. **72**(4), 351–368 (2015). https://doi.org/10.5505/TurkHijyen.2015.09581
2. G. Donzelli, R. Gehring, S. Murugadoss, T. Roos, A. Schaffert, N. Linzalone, A critical review on the toxicological and epidemiological evidence integration for assessing human health risks to environmental chemical exposures. Rev. Environ. Health. (2024). https://doi.org/10.1515/reveh-2024-0072
3. W. Zhou, M.M. Li, V. Achal, A comprehensive review on environmental and human health impacts of chemical pesticide usage. Emerg. Contaminants. **11**(1) (2025). https://doi.org/10.1016/j.emcon.2024.100410
4. R. Lafi, L. Gzara, R.H. Lajimi, A. Hafiane, Treatment of textile wastewater by a hybrid ultrafiltration/electrodialysis process. Chem. Eng. Process. - Process. Intensif. **132**, 105–113 (2018). https://doi.org/10.1016/j.cep.2018.08.010
5. K. Vigneswaran, S. Neill, C.G. Hadjipanayis, Beyond the world health organization grading of infiltrating gliomas: advances in the molecular genetics of glioma classification. Ann. Transl Med. **3**(7), 95 (2015). https://doi.org/10.3978/j.issn.2305-5839.2015.03.57
6. O. Deveoglu, R. Karadag, A review on the flavonoids -A dye source Doğal Boya Kaynağı -Flavonoidler Üzerine Derleme. Int. J. Adv. Eng. Pure Sci. **31** (2019). https://doi.org/10.7240/jeps.476514
7. S. Dutta, S. Adhikary, S. Bhattacharya, D. Roy, S. Chatterjee, A. Chakraborty, D. Banerjee, A. Ganguly, S. Nanda, P. Rajak, Contamination of textile dyes in aquatic environment: adverse impacts on aquatic ecosystem and human health, and its management using bioremediation. J. Environ. Manage. 353 (2024). https://doi.org/10.1016/j.jenvman.2024.120103
8. H. Kolya, C.W. Kang, Toxicity of metal oxides, dyes, and dissolved organic matter in water: implications for the environment and human health. Toxics. **12**(2) (2024). https://doi.org/10.3390/toxics12020111
9. G. Yentür, Investigation of the amount of synthetic dye in cake decorations and some candies provided from Ankara markets.

Ankara Univ. J. Veterinary Med. Fac. **43**(01) (1996). https://doi.org/10.1501/Vetfak_0000000712
10. S. Bisht, K.K. Gaikwad, Natural Pigments or Dyes for Sustainable Food Packaging Application, food and bioprocess technology (2025). https://doi.org/10.1007/s11947-025-03756-2
11. G. Sudhakaran, Artificial food dyes are toxic: neurobehavioral implications in children. Brain Spine. **4** (2024). https://doi.org/10.1016/j.bas.2024.102869
12. S. Yadav, K.S. Tiwari, C. Gupta, M.K. Tiwari, A. Khan, S.P. Sonkar, A brief review on natural dyes, pigments: recent advances and future perspectives. Res. Chem. **5**, 100733 (2023). https://doi.org/10.1016/j.rechem.2022.100733
13. L. Chungkrang, S. Bhuyan, Natural dye sources and its applications in textiles: A brief review. Int. J. Curr. Microbiol. Appl. Sci. **9**(10), 261–269 (2020). https://doi.org/10.20546/ijcmas.2020.910.034
14. I. Surowiec, J. Orska-Gawryś, M. Biesaga, M. Trojanowicz, M. Hutta, R. Halko, K. Urbaniak-Walczak, Identification of natural dyestuff in archeological Coptic textiles by HPLC with fluorescence detection. Anal. Lett. **36**(6), 1211–1229 (2003). https://doi.org/10.1081/AL-120020154
15. A. Ammasi, R. Iruthayaraj, A.P. Munusamy, M. Shkir, Enhancement of highly efficient flavone-based organic dyes with different anchoring groups effect in dye-sensitized solar cells using experimental and TD-DFT study. J. Mater. science-materials Electron. **34**(17) (2023). https://doi.org/10.1007/s10854-023-10736-9
16. H. Roohi, V. Pourghasem, Exploring the photophysical properties of flavone-based dyes as an anti-angiogenic agent and with fluorescence emission in the near-infrared (NIR) region: a TD-DFT study. Mol. Phys. **122**(18) (2024). https://doi.org/10.1080/00268976.2024.2317451
17. J.K. Kumar, A.K. Sinha, Resurgence of natural colourants: a holistic view. Nat. Prod. Res. **18**(1), 59–84 (2004). https://doi.org/10.1080/1057563031000122112
18. I. Surowiec, A. Quye, M. Trojanowicz, Liquid chromatography determination of natural dyes in extracts from historical Scottish textiles excavated from peat bogs. J. Chromatogr. A **1112**(1), 209–217 (2006). https://doi.org/10.1016/j.chroma.2005.11.019
19. L.V. Aswanilal, E.A. Siril, Enhanced production of Alizarin type anthraquinone dye achieved through biotransformation of Oldenlandia umbellata L. using different strains of Agrobacterium rhizogenes. Plant. Cell. Tissue Organ. Cult. **160**(1) (2025). https://doi.org/10.1007/s11240-024-02956-6
20. S. Bin Shabbir, S.A. Khan, M. Khan, J.U. Din, S. Irshad, M.H. Mahmoud, A. Qadeer, M. Hamayun, Characterization of partially purified manganese peroxidase from Soil-Derived Aspergillus species and its biodegradation potential against Anthraquinone-Based dye. Ind. Biotechnol. **21**(1), 36–46 (2025). https://doi.org/10.1089/ind.2024.0040
21. H. Heryanto, D. Tahir, Trends, mechanisms, and the role of advanced oxidation processes in mitigating Azo, triarylmethane, and anthraquinone dye pollution: A bibliometric analysis. Inorg. Chem. Commun. **175** (2025). https://doi.org/10.1016/j.inoche.2025.114104
22. E.M. Malik, C.E. Müller, Anthraquinones as Pharmacological tools and drugs. Med. Res. Rev. **36**(4), 705–748 (2016). https://doi.org/10.1002/med.21391
23. T.H. Le, M.H. Nguyen, A.L.T. Le, M.T.T. Nguyen, H.X. Nguyen, T.N.V. Do, N.T. Nguyen, In Vitro Biological Evaluation and In Silico Studies of a New Anthraquinone From <i>Zingiber Cassumunar Roxb. in Type 2 Diabetes Management, Chem. Biodivers. (2025). https://doi.org/10.1002/cbdv.202403129
24. S.K. Lee, J.W. Keng, J.A. Yon, C.W. Mai, H.C. Lim, S.C. Chow, G.A. Akowuah, K.B. Liew, S.K. Lee, P.J. Marriott, Y.L. Chew, Phytochemical analysis and biological activities of flavonoids and anthraquinones from Cassia Alata (Linnaeus) Roxburgh and their implications for atopic dermatitis management. Plants-Basel. **14**(3) (2025). https://doi.org/10.3390/plants14030362
25. S.S. Wu, X.P. Zhou, F. Li, W. Sun, Q.C. Zheng, D. Liang, Novel Anthraquinone-Based Benzenesulfonamide Derivatives and Their Analogues as Potent Human Carbonic Anhydrase Inhibitors with Antitumor Activity: Synthesis, Biological Evaluation, and In Silico Analysis, Int. J. Mol. Sci. 25(6) (2024). https://doi.org/10.3390/ijms25063348
26. M. Maqsood, N. Shafiq, M.T. Hussain, Novel pyrimidine-anthraquinone dyes: design, synthesis, textile applications & their computational SAR analysis. J. Mol. Struct. **1321** (2025). https://doi.org/10.1016/j.molstruc.2024.140096
27. S.M. Mugo, W.H. Lu, S. Robertson, Anthraquinone-Polyaniline-Integrated textile platforms for in situ electrochemical production of hydrogen peroxide for microbial deactivation. Polymers. **15**(13) (2023). https://doi.org/10.3390/polym15132859
28. L.A. Thompson, W.S. Darwish, Environmental Chemical Contaminants in Food: Review of a Global Problem, J Toxicol 2019 (2019) 2345283. https://doi.org/10.1155/2019/2345283
29. Z. Koksal, R. Kalin, P. Kalin, M. Karaman, İ. Gulcin, H. Ozdemir, Lactoperoxidase Inhibition of some natural phenolic compounds: kinetics and molecular Docking studies. J. Food Biochem. **44**(2), e13132 (2020). https://doi.org/10.1111/jfbc.13132
30. E. Grun, Importance of lactoperoxidase-thiocyanate-peroxide system (lps) to bacteria content of cow milk. Monatshefte Fur Veterinarmedizin. **39**(20), 693–698 (1984)
31. S. Bayrak, S. Gerni, C. Öztürk, Z. Almaz, Ç. Bayrak, N. Kilincç, H. Özdemir, Lactoperoxidase Inhibition of celecoxib derivatives containing the pyrazole Linked-Sulfonamide moiety: antioxidant capacity, antimicrobial activity, and molecular Docking studies. J. Biochem. Mol. Toxic. **38**(11) (2024). https://doi.org/10.1002/jbt.70055
32. Z. Köksal, P. Güller, A. Keskin, Lactoperoxidase Inhibition by some carnosol and carnosic acid derivatives: in vitro, in Silico and statistical approaches. Food Bioscience. **62** (2024). https://doi.org/10.1016/j.fbio.2024.105485
33. B. Reiter, Review of the progress of dairy science: antimicrobial systems in milk, J Dairy Res 45(1) (1978) 131–47. https://doi.org/10.1017/s0022029900016290
34. N. Abul, S. Gerni, I.N. Korkmaz, Y. Demir, H. Özdemir, İ. Gülçin, Screening of in vitro Inhibition of lactoperoxidase enzyme by Methyl benzoate derivatives with molecular Docking studies. Chem. Biodivers. **20**(8), e202300687 (2023). https://doi.org/10.1002/cbdv.202300687
35. J.S. Shindler, W.G. Bardsley, Steady-state kinetics of lactoperoxidase with ABTS as chromogen. Biochem. Biophys. Res. Commun. **67**(4), 1307–1312 (1975). https://doi.org/10.1016/0006-291x(75)90169-2
36. H. Özdemir, M.T. Uğuz, In vitro effects of some anaesthetic drugs on lactoperoxidase enzyme activity. J. Enzym Inhib. Med. Chem. **20**(5), 491–495 (2005). https://doi.org/10.1080/14756360500225045
37. K. Awol, M. Taye, B. Kassa, Activation of lactoperoxidase system and its potential for microbial Inhibition and preservation of milk in the great African rift Valley climate. COGENT FOOD Agric. **9**(1) (2023). https://doi.org/10.1080/23311932.2023.2247691
38. R. Kalin, Z. Köksal, S. Bayrak, S. Gerni, I.N. Ozyürek, H. Usanmaz, M. Karaman, A. Atasever, H. Özdemir, I. Gülçin, Molecular Docking and Inhibition profiles of some antibiotics on lactoperoxidase enzyme purified from bovine milk. J. Biomol. Struct. Dyn. **40**(1), 401–410 (2022). https://doi.org/10.1080/07391102.2020.1814416
39. H. Lineweaver, D. Burk, The determination of enzyme dissociation constants. J. Am. Chem. Soc. **56**(3), 658–666 (1934). https://doi.org/10.1021/ja01318a036

40. H. Şenol, F. Çakır, 3-Amino-thiophene-2-carbohydrazide Derivatives as Anti Colon Cancer Agents: Synthesis, Characterization, In-Silico and In-Vitro Biological Activity Studies, ChemistrySelect 8(39) (2023) e202302448. https://doi.org/10.1002/slct.202302448
41. Ö. Demirkıran, E. Erol, H. Şenol, İ.M. Kesdi, G.Ö. Alim Toraman, E.Ş. Okudan, G. Topcu, Cytotoxic meroterpenoids from brown Alga Stypopodium schimperi (Kützing) verlaque & Boudouresque with comprehensive molecular Docking & dynamics and ADME studies. Process Biochem. **136**, 90–108 (2024). https://doi.org/10.1016/j.procbio.2023.11.029
42. F.S. Tokalı, H. Şenol, H.I. Yetke, E. Hacıosmanoğlu-Aldogan, Novel quinazoline-chromene hybrids as anticancer agents: synthesis, biological activity, molecular docking, dynamics and ADME studies. Arch. Pharm. **356**(11), e2300423 (2023). https://doi.org/10.1002/ardp.202300423
43. B. Zengin Kurt, D. Öztürk Civelek, E.B. Çakmak, Y. Kolcuoğlu, H. Şenol, B.N. Sağlık Özkan, A. Dag, K. Benkli, Synthesis of Sorafenib–Ruthenium complexes, investigation of biological activities and applications in drug delivery systems as an anticancer agent. J. Med. Chem. **67**(6), 4463–4482 (2024). https://doi.org/10.1021/acs.jmedchem.3c01115
44. H. Şenol, 4-Furfuryloxymethyl-1,2,3-triazol-1-yl-acetohydrazide Hybrids as Cholinesterase and Carbonic Anhydrase Inhibitors: Synthesis, Characterization and Comprehensive Biological Activity Studies, ChemistrySelect 9(6) (2024) e202303927. https://doi.org/10.1002/slct.202303927
45. F.S. Tokalı, H. Şenol, Ş. Ateşoğlu, P. Tokalı, F. Akbaş, Exploring highly selective polymethoxy Fenamate isosteres as novel antiprostate cancer agents: synthesis, biological activity, molecular docking, molecular dynamics, and ADME studies. J. Mol. Struct. **1319**, 139519 (2025). https://doi.org/10.1016/j.molstruc.2024.139519
46. Z. Arslan, E. Okuroğlu, H. Şenol, Z. Türkmen, 1-Benzhydrylpiperazine: isolation, structure determination, and in Silico studies for a novel potential narcotic agent detected in sports supplements. J. Food Compos. Anal. 106682 (2024). https://doi.org/10.1016/j.jfca.2024.106682
47. F. Göç, A. Sarı, H. Şenol, N. Özsoy, S. Makbul, K. Coşkunçelebi, Bioactive Phenolic Contents of Scorzonera ketzkhowelii Sosn. ex Grossh. (Asteraceae) with Comprehensive In vitro and In silico Studies, J. Mol. Struct. (2024) 140436. https://doi.org/10.1016/j.molstruc.2024.140436
48. J. Eshal, H.Z. Tariq, J. Li, H. Aftab, H. Şenol, P. Taslimi, N. Sadeghian, R.D. Alharthy, M.S. Akram, R. Talib, Z. Shafiq, Synthesis, biological evaluation, and in Silico studies of phenyl naphthalene-2-sulfonate derived thiosemicarbazones as potential carbonic anhydrase inhibitors. Bioorg. Chem. **155**, 108118 (2025). https://doi.org/10.1016/j.bioorg.2024.108118
49. A. Akıncıoğlu, Y. Akbaba, H. Göçer, S. Göksu, İ. Gülçin, C.T. Supuran, Novel sulfamides as potential carbonic anhydrase isoenzymes inhibitors. Bioorg. Med. Chem. **21**(6), 1379–1385 (2013). https://doi.org/10.1016/j.bmc.2013.01.019
50. Y. Demir, Naphthoquinones, benzoquinones, and anthraquinones: molecular docking, ADME and Inhibition studies on human serum paraoxonase-1 associated with cardiovascular diseases. Drug Dev. Res. **81**(5), 628–636 (2020). https://doi.org/10.1002/ddr.21667
51. B. Gökçe, Investigation effects of some anthraquinones on human paraoxonase 1 (hPON1), Balıkesir Üniversitesi Fen bilimleri. Enstitüsü Dergisi. **21**(2), 546–553 (2019). https://doi.org/10.25092/baunfbed.624457
52. V. Boháčová, P. Dočolomanský, A. Breier, P. Gemeiner, A. Ziegelhöffer, Interaction of lactate dehydrogenase with anthraquinone dyes: characterization of ligands for dye–ligand chromatography. J. Chromatogr. B Biomed. Sci. Appl. **715**(1), 273–281 (1998). https://doi.org/10.1016/S0378-4347(98)00088-7
53. H.E. Duran, Ş. Beydemir, Naphthoquinones and anthraquinones: exploring their impact on acetylcholinesterase enzyme activity. Biotechnol. Appl. Chem. **71**(5), 1079–1093 (2024). https://doi.org/10.1002/bab.2599
54. T.I. Adelusi, A.-Q.K. Oyedele, I.D. Boyenle, A.T. Ogunlana, R.O. Adeyemi, C.D. Ukachi, M.O. Idris, O.T. Olaoba, I.O. Adedotun, O.E. Kolawole, Y. Xiaoxing, M. Abdul-Hammed, Molecular modeling in drug discovery. Inf. Med. Unlocked. **29**, 100880 (2022). https://doi.org/10.1016/j.imu.2022.100880
55. S. Saikia, M. Bordoloi, Challenges, advances and its use in drug discovery perspective. Curr. Drug Targets. **20**(5), 501–521 (2019). https://doi.org/10.2174/1389450119666181022153016
56. A. Atasever, H. Ozdemir, I. Gulcin, O. Irfan, Kufrevioglu, One-step purification of lactoperoxidase from bovine milk by affinity chromatography. Food Chem. **136**(2), 864–870 (2013). https://doi.org/10.1016/j.foodchem.2012.08.072